

# Development and Analysis of a Wearable Biopatch for Electrocardiogram Monitoring and Hydration Assessment

Jiho Jun<sup>1</sup>, Woon-Hong Yeo<sup>#</sup> and Taewoog Kang<sup>#</sup>

<sup>1</sup>Lambert High School, USA

<sup>#</sup>Advisor

## ABSTRACT

Biopatch is emerging as an innovative device in the field of health monitoring. The goal of this article is to create an adhesive biopatch that can be applied to the user's skin to measure electrocardiogram (ECG), body temperature, and inertial measurement unit (IMU) data. Then, sets of data are then collected in four different environments: running with and without water intake, and resting with and without water intake. In this case, the ECG data was analyzed to indicate the user's hydration state. Future applications of this data involve the integration of machine learning algorithms to predict hydration levels, contributing to essential health monitoring. Although this technology has the potential to improve personal healthcare, more research and technological advancement are needed to reach its full potential.

## Introduction

Biopatch is a small, adhesive device that could redefine personal health monitoring. While patches might seem simple, this one goes beyond just sticking to your skin; it bridges the gap between biology and technology, creating a bio-interfaced tool that could be vital for our well-being.<sup>1</sup>

The biopatch is designed to monitor key physiological signals, including ECG, body temperature, and IMU, offering a non-invasive way to assess a user's health in real-time.<sup>2</sup> Whether you're running a marathon, resting after a workout, or simply going about your daily life, this device can provide crucial data on your hydration state—a vital indicator of overall health. By tracking these signals in different scenarios, such as exercising with and without water intake, the biopatch aims to detect imbalances that could indicate dehydration or electrolyte deficiencies.<sup>3</sup>

This article explores the development and potential applications of the biopatch, investigating its ability to collect and analyze data. The article also examines how machine learning could be leveraged to predict hydration levels, offering a glimpse into the future of personalized healthcare.<sup>4</sup>

## Materials

Wearable electronics, such as the biopatch, have become increasingly essential for health monitoring due to their ability to provide real-time, continuous data in a non-invasive manner.<sup>1</sup> In this research, the biopatch was designed as a lightweight (6.5 g), flexible, and compact wearable health monitoring device, measuring 8.5 cm × 4.0 cm, with an adhesive thickness of 0.28 mm and a module thickness of 3.0 mm. Its form factor allowed for ease of use without requiring additional tools or specialized training, making it highly accessible for general users in environments where continuous physiological monitoring is critical.<sup>2</sup>



At the core of the biopatch was a wireless sensor module powered by a 105 mAh lithium-ion polymer battery (LP401230, Adafruit), designed for low-power, long-term use. The wireless capabilities of this module enabled seamless data collection without restricting the wearer's movement, a crucial factor in real-time monitoring applications.<sup>2</sup> The sensor module integrated several key components for sensing, signal processing, and wireless data transmission. Specifically, it houses an analog-to-digital converter (ADC, ADS1292, Texas Instruments) to capture ECG signals, a digital temperature sensor (TMP117, Texas Instruments) with  $\pm 0.1$  °C accuracy for body temperature monitoring, and a motion sensor (ICM-20948, TDK Corporation) to detect linear and angular acceleration along three axes at 50 Hz.<sup>2</sup> All these components were managed by a System-on-Chip module (nRF52832, Nordic Semiconductors), which processed the data and transmits it via Bluetooth Low Energy (BLE) to an Android smartphone for real-time analysis and storage.<sup>3</sup>

The ECG monitoring functionality of the biopatch was designed to capture and analyze physiological signals in real-time, a capability increasingly relevant in clinical and research settings. The soft, flexible design of the device allowed for improved adherence to the skin, particularly during prolonged usage in activities such as exercise monitoring.<sup>4</sup>

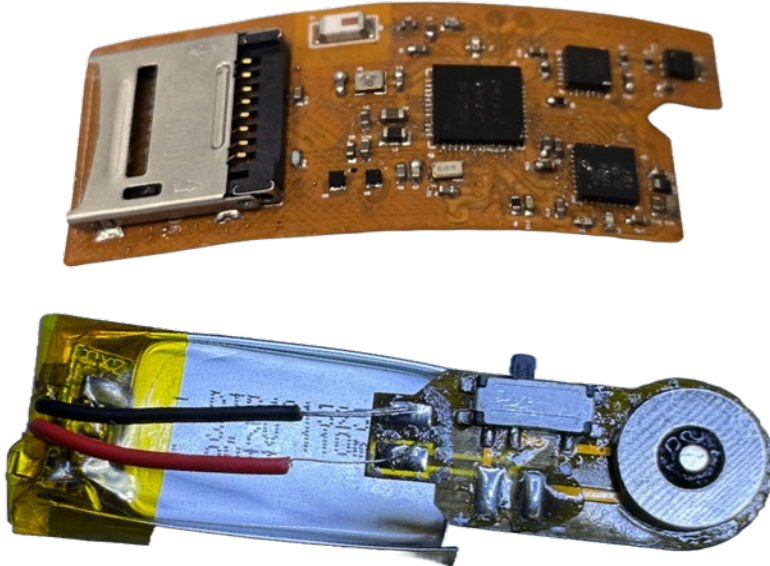


**Figure 1.** Wireless Sensor Module and Lithium-Ion Battery

## Fabrication and Assembly of Biopatch

### Fabrication of Electrodes

The fabrication of the biopatch's flexible electronics leveraged advanced microfabrication techniques to ensure durability and flexibility. The ECG electrodes were deposited with chromium (5 nm) and copper (200 nm) using micro-fabrication techniques similar to those used in other soft bioelectronics applications.<sup>5</sup> The electrodes were then patterned using a femtosecond infrared laser micromachining system (WS-Flex, Optec), a technique known for its precision in creating complex geometries while maintaining material integrity.<sup>2</sup> This method allowed for the laser cutting of electrodes in a serpentine pattern on a 12.7  $\mu$ m thick polyimide substrate (Kapton 50HN, DuPont), which enhanced mechanical stretchability. The serpentine design was a strategy for ensuring that the electrodes can stretch by up to

30% without electrical failure, a crucial feature for continuous monitoring in high-motion environments, such as exercise or everyday activities.<sup>4</sup>

### Fabrication of Adhesive Tape

Once the polyimide substrate with the electrodes was fabricated, it was laminated onto a silicone elastomer (Ecoflex 0030, Smooth-On). The use of Ecoflex ensured that the biopatch remained flexible and stretchable while providing insulation and protection for the sensitive electronic components. The electrodes were then integrated directly into the adhesive side of 3M 9907T medical-grade tape, which is breathable and promotes robust skin-electrode contact.<sup>3</sup> This integration ensured that the electrodes remain securely attached to the skin, even during periods of sweating or physical activity. To further protect the module from environmental factors such as dust, sweat, and friction from clothing, an additional layer of smaller cover tape was applied over the module.<sup>2</sup>

### Assembly

During the assembly process, the wireless sensor module and the lithium-ion battery were securely bonded using superglue, ensuring compact integration of the power source with the electronics. This compact integration was crucial for maintaining the flexibility of the biopatch while minimizing bulk.<sup>2</sup> Ecoflex was applied to attach the combined module and battery to the adhesive tape, ensuring a durable yet flexible bond. The electrode tip was then soldered to the backside of the module to optimize signal transmission from the skin to the processing unit.

After the assembly was completed, the biopatch underwent an oven-curing process for 20 minutes, which ensured that the materials were fully set and that the mechanical integrity of the final product was stable. This process allowed the biopatch to withstand environmental stresses and ensured its functionality in both resting and active conditions. The final product, as shown in Figure 2, is a compact, wearable patch capable of continuous monitoring and resistant to environmental conditions.



**Figure 2.** Assembled Biopatch

## Data Acquisition and Processing

### Data Acquisition

#### *Experiment Overview*

To evaluate the biopatch's effectiveness in measuring ECG signals under different hydration conditions, two treadmill experiments were conducted on separate days. The primary aim was to gather ECG data in four distinct scenarios: running without drinking water, running with drinking water, resting without drinking water, and resting with drinking water. These conditions mimic real-world situations where hydration levels affect physiological performance, particularly heart function.

The treadmill experiments were structured as follows:

Experiment 1 (No Water):

30 min incline at 3°, 4°, and 4.5°  
30 min rest  
30 min incline at 4.5°  
5 min rest  
30 min incline at 4.5°  
10 min standing

In this experiment, no water was consumed throughout the running and resting periods to simulate a dehydrated state. The goal was to observe how a lack of hydration affects the ECG signals during both activity and rest phases.

Experiment 2 (With Water):

30 min incline at 3°, 4°, and 4.5° (water intake every 5 minutes, experiment stopped at ~1870 seconds)  
30 min rest (water intake as needed)  
30 min incline at 4.5° (water intake as needed)  
5 min rest  
30 min incline at 4.5° (water intake as needed)  
10 min standing (water intake as needed)

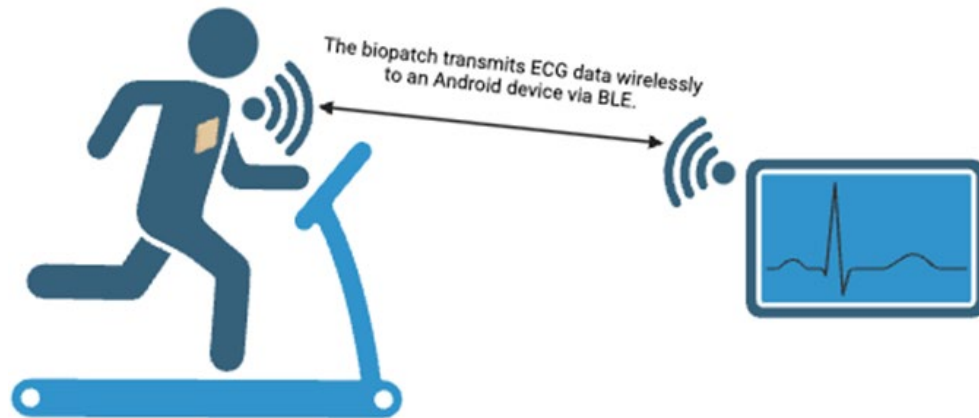
In this second experiment, water was consumed at regular intervals, with hydration provided every 5 minutes during running. The resting period also allowed for water intake at the participant's discretion, mimicking a hydrated state.

#### *During Experiment*

ECG data were collected continuously throughout the treadmill sessions using a custom biopatch. The signals were transmitted wirelessly to an Android smartphone, where they were stored in CSV format for further analysis. The ECG data were recorded at a sampling rate of 250 Hz, providing high temporal resolution to capture the detailed morphology of the cardiac cycle. In addition to the ECG signals, body temperature and motion data were collected simultaneously to provide context for interpreting physiological responses, particularly hydration status.

The data collection resulted in four distinct datasets:

- Running without drinking water
- Running with drinking water
- Resting without drinking water
- Resting with drinking water



Created in BioRender.com 

**Figure 3.** Wireless ECG Monitoring during Exercise using a Wearable Biopatch. Created with BioRender.com

### Data Processing in MATLAB

Once the raw ECG data were obtained, they were preprocessed in MATLAB to remove noise and artifacts, making them suitable for detailed analysis. The signals were initially loaded from the CSV files and subjected to a series of filtering techniques designed to clean and standardize the data. A notch filter was first applied to remove powerline interference at 60 Hz, a common source of electrical noise in biomedical signals.<sup>6 7</sup> This process effectively eliminated external noise without distorting the ECG signal, preserving the integrity of the data for further analysis.<sup>8</sup>

Following this, a bandpass filter was implemented to isolate the specific frequency range relevant to the ECG signal, while reducing baseline wander and high-frequency noise.<sup>6</sup> This step ensured the retention of critical ECG components, such as the QRS complex, T-wave, and P-wave, while discarding irrelevant noise.<sup>7</sup> Additionally, a baseline drift removal filter was used to correct for slow signal variations caused by subject movement or respiration, a frequent issue in real-world physiological data collection.<sup>8</sup> This process ensured the stability of the ECG signal, allowing for clearer interpretation of the underlying cardiac activity.<sup>9</sup>

After filtering, the ECG signals were normalized by scaling them to a consistent range. This normalization allowed for more accurate comparisons across different sessions and subjects by minimizing amplitude variations caused by differences in electrode placement or skin conductivity.<sup>10</sup> The signals were scaled between 0 and 1, using the minimum and maximum values within each dataset to maintain consistency.

Once preprocessing was complete, the ECG signals were segmented into time windows, allowing for comparisons between experimental conditions such as running versus resting, and hydrated versus dehydrated states. MATLAB was then used to extract key features from the ECG signals, including R-R intervals and the morphology of the QRS complex.<sup>11</sup> These features were further analyzed to identify patterns that could indicate changes in hydration status, such as increased heart rate variability and altered QRS morphology under dehydrated conditions.<sup>12 13</sup>

By applying these signal processing techniques, the ECG data were prepared for additional statistical analyses, enabling the assessment of physiological impacts related to hydration and physical exertion during exercise.

### ECG Signal Generation

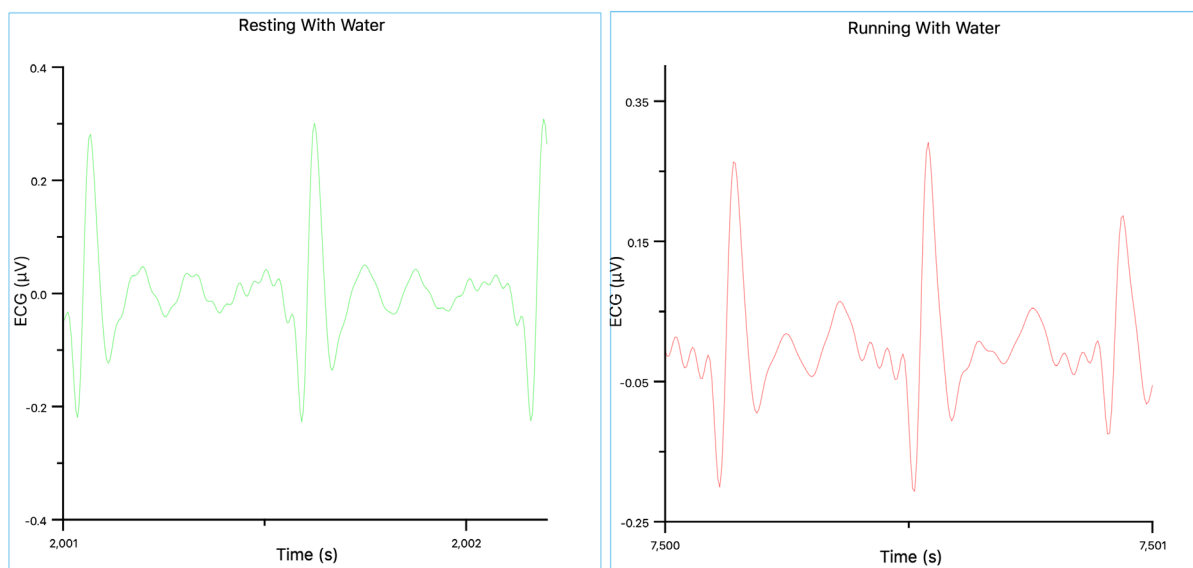
After the data had been processed, the CSV files generated from the wearable biopatch were imported into Labplot2 for visual representation. Time vectors were created to represent the duration of each recording session, and these vectors were combined with the processed ECG signals.<sup>8 9</sup> The data were plotted using Labplot's built-in graphing capabilities, which resulted in the creation of detailed ECG graphs that depicted the heart's electrical activity over time for each subject and condition.

These visual representations in Labplot2 provided clear comparisons between different hydration and activity states. In each dataset, key features of the ECG waveforms, including P-waves, QRS complexes, and T-waves, were prominently displayed.<sup>6 12</sup> These features allowed for the observation of the heart's electrical response under varying conditions, offering valuable insights into how hydration impacts cardiac function.<sup>13 14</sup> The consistency and clarity of the graphs facilitated the identification of crucial ECG markers, such as R-peaks, which were used for the analysis of heart rate and heart rate variability.<sup>5</sup>

The graphical representation of the ECG data laid a strong foundation for further analysis and interpretation, allowing for an in-depth assessment of how hydration affects cardiac performance during physical exercise.

### Analysis of ECG Patterns

The ECG data were segmented into four different datasets, each representing a specific combination of hydration and activity: Green (resting with drinking water), Red (running with drinking water), Blue (resting without drinking water), and Pink (running without drinking water).



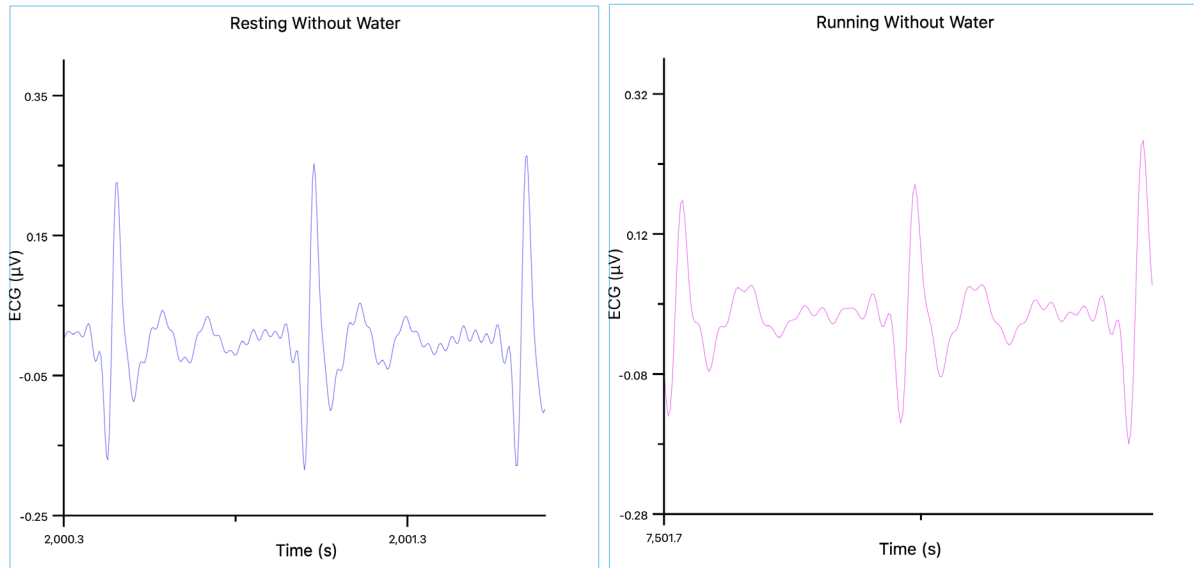


**Figure 4.** Segments of ECG of 4 different datasets. The first graph (green) refers to resting with drinking water, the second graph (red) refers to running with drinking water, the third graph (blue) refers to resting without drinking water, and the fourth graph (pink) refers to running without drinking water. Created with Labplot2.

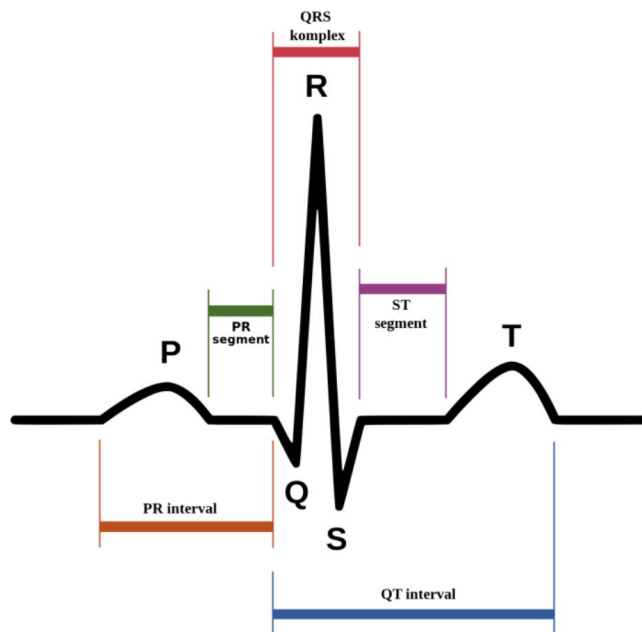


**Figure 5.** Labeled ordinary ECG graph. For reference.

Clear differences in the ECG waveforms were observed between four conditions, highlighting the impact of hydration and physical exertion on cardiac function. The analysis focused on the key components of the ECG waveform, namely the P-wave, QRS complex, and T-wave, to understand the physiological responses to hydration and activity levels.<sup>12</sup>

## QRS Complex

The QRS complex, which represents ventricular depolarization, displayed clear variability between the hydrated and dehydrated states, highlighting the impact of hydration on cardiac performance. In the first and second graph, the QRS complexes were well-defined and consistent, indicating stable cardiac function.<sup>12</sup> Even during running, the second graph exhibited a regular QRS complex, suggesting that hydration allowed the heart to efficiently manage the increased physical activity.<sup>13</sup>

In contrast, the QRS complexes of the third and fourth graph displayed irregularities. Specifically, in the fourth graph, the amplitude of the QRS complex showed greater variability, a likely indication of cardiovascular strain due to dehydration.<sup>14</sup> This increased variability suggests that the heart, while under physical exertion, struggled to maintain effective circulation without adequate hydration, consistent with previous findings on the physiological effects of dehydration.<sup>15</sup>

## T-Wave

The T-wave, representing ventricular repolarization, also showed notable differences across the datasets. In the hydrated conditions, both the first and second graph demonstrated smooth and consistent T-waves, reflecting efficient ventricular recovery.<sup>16</sup> Even during the running phase in the second graph, the T-wave remained relatively stable, indicating that hydration helped maintain normal repolarization processes despite the physical load.<sup>16</sup>

However, subtle abnormalities were observed in the T-waves of the third and fourth graphs. In the third graph, the T-wave appeared slightly flattened, which may signal early signs of electrolyte imbalance that are commonly associated with dehydration.<sup>17</sup> These abnormalities were more pronounced in the fourth graph, where the T-wave not only appeared flattened but also exhibited slight irregularities. This suggested that the cardiovascular strain associated with dehydration was exacerbated by physical exertion, impairing the heart's repolarization process.<sup>6</sup>

## P-Wave

The P-wave, which reflects atrial depolarization, was generally stable across the subjects. However, in the dehydrated subjects, minor reductions in the amplitude of the P-wave were observed. This may indicate reduced atrial efficiency, a known effect of dehydration due to decreased blood volume and electrolyte imbalances.<sup>18</sup> In contrast, hydrated subjects exhibited more stable and consistent P-waves, suggesting that hydration supported normal atrial function even under the increased demands of physical activity.<sup>13 15</sup>

## Heart Rate and R-R Interval

The heart rate, as inferred from the R-R interval (the time between consecutive R-peaks), revealed significant differences between the hydrated and dehydrated subjects. In the first graph, the R-R intervals were long and regular, corresponding to a stable and slower heart rate, indicative of normal resting conditions.<sup>6</sup> Similarly, the second graph showed relatively consistent R-R intervals, even though the heart rate increased with physical exertion. This consistency highlighted the stabilizing effect of hydration on cardiac performance under stress.<sup>15</sup>

On the other hand, the third graph exhibited shorter and more variable R-R intervals, reflecting an elevated heart rate even at rest, a typical response to dehydration.<sup>15</sup> In the fourth graph, this variability was even more pronounced, with highly irregular R-R intervals and a significantly elevated heart rate. These findings align with the known physiological effects of dehydration, where reduced blood volume forces the heart to work harder, leading to increased heart rate variability and reduced efficiency.<sup>16</sup>

## Comparative Patterns

In summary, the ECG waveforms of the hydrated subjects were smoother and more consistent, with well-defined QRS complexes, T-waves, and P-waves. These findings suggest that adequate hydration helped maintain normal cardiac function, even during physically demanding activities like running.<sup>14</sup> Conversely, the ECG patterns in the dehydrated subjects displayed significant irregularities, particularly in the QRS complex and T-wave, reflecting increased cardiovascular stress.<sup>14 15</sup> The elevated heart rate variability and subtle changes in waveform morphology observed in these subjects further illustrate the reduced efficiency of the heart under dehydrated conditions.<sup>15</sup> These findings underscore the critical role of hydration in maintaining normal cardiac function during physical activity and highlight the potential for ECG monitoring to detect early signs of dehydration and cardiovascular strain.

## Validations of ECG Analysis

The additional data collected from the biopatch further validated the observed differences in ECG between hydrated and dehydrated states. Heart rate (HR) data showed that water intake leads to a lower HR during exercise and a quicker recovery to baseline during rest periods, which was consistent with established insights on hydration's role in maintaining cardiovascular stability.<sup>19</sup> Without water, HR was higher and more variable, indicative of cardiovascular strain during dehydration.<sup>19</sup> Additionally, the motion data showed comparable levels of physical activity across conditions, ensuring that observed differences are primarily due to hydration rather than variations in exertion levels. Temperature data further demonstrated that hydration supports more effective thermal regulation during exercise, with lower temperature curves in hydrated states.<sup>20</sup> These findings emphasized the importance of proper hydration for cardiovascular and thermal stability during physical activity, helping to reduce the physiological strain of exercise.<sup>20</sup>

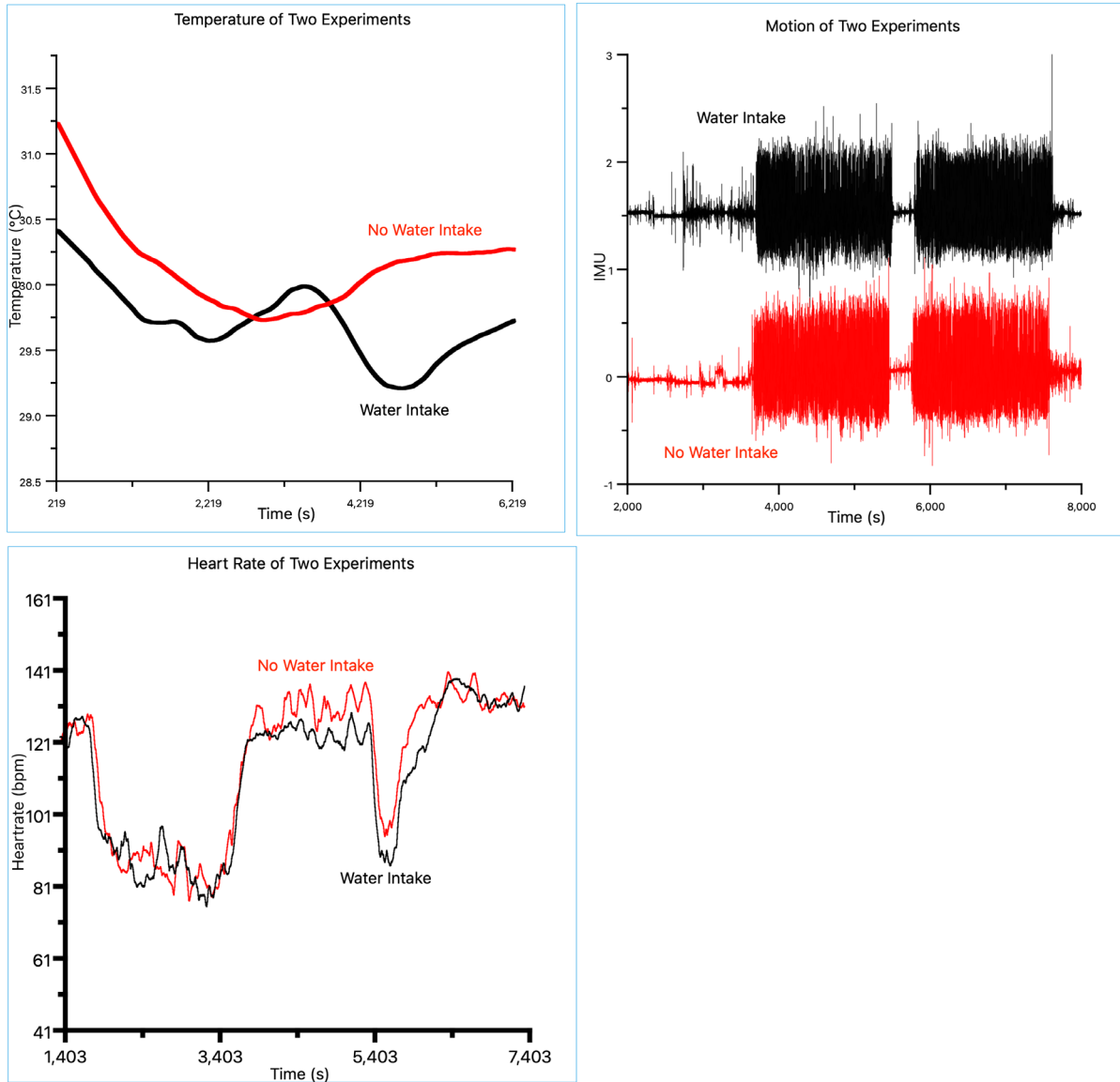


**Figure 6.** Graphs of Temperature, Inertial Measurement Units, and Heart Rate throughout the two experiments.

## Potential Applications

The distinct ECG patterns observed across the four datasets offer a robust foundation for applying machine learning algorithms to predict a user's hydration state and detect potential electrolyte imbalances. By leveraging key features such as R-R intervals, QRS complex variability, and T-wave morphology, neural networks can be trained to assess hydration levels based on real-time physiological signals.<sup>12-10</sup> For example, the increased heart rate variability and altered QRS complex observed in dehydrated subjects could serve as crucial predictors for identifying dehydration.<sup>15</sup> Such machine learning models could be applied in various fields, including sports and fitness, where maintaining proper hydration is vital to athletic performance and recovery.<sup>20</sup> Occupational health in physically demanding environments, such as construction or agriculture, could also benefit from real-time hydration monitoring to prevent dehydration-related injuries.<sup>2</sup>

In addition to hydration monitoring, the ECG abnormalities seen in T-wave flattening and QRS complex variability under dehydrated conditions open the door to detecting electrolyte imbalances such as hyperkalemia and hypokalemia.<sup>21</sup> Machine learning algorithms can be trained to recognize these subtle ECG markers, allowing for early detection and intervention before severe symptoms arise.<sup>12</sup> The integration of such predictive capabilities into wearable devices, like the biopatch, could revolutionize healthcare by providing continuous, non-invasive monitoring of electrolyte levels and cardiac health. These advancements have the potential to reduce the incidence of dangerous cardiac events, particularly in at-risk populations, and support early diagnosis and intervention in real-world settings.<sup>3</sup>

## Conclusion

The biopatch demonstrated its capability to monitor ECG signals and detect differences in heart function based on hydration states. Analysis of data obtained in four various conditions showed distinct differences in the QRS complex, T-wave, and heart rate variability. These results demonstrate the critical role that water plays in preserving circulatory stability, with dehydrated conditions exhibiting more strain and variability. Additionally, validation of ECG analysis using additional data confirmed the accuracy of the biopatch's measurements. The research mainly concentrated on data gathering, signal preprocessing, and ECG waveform analysis to distinguish between hydrated and dehydrated conditions.

Finally, the incorporation of machine learning algorithms holds promise for further improving this technology. Future uses could allow real-time hydration state prediction and early electrolyte imbalance diagnosis by training models to recognize hydration-related patterns in ECG data. Personalized healthcare could be greatly enhanced by this wearable technology and machine learning, especially in areas like sports, fitness, and occupational health.

## Acknowledgments

I would like to thank Prof. Yeo and Dr. Kang for providing me with spaces to research and experiment, helping me brainstorm, and giving invaluable insights into the topic. Their guidance throughout the experimental process allowed me to push the boundaries of my research and think critically about each phase of the project.

## References

1. Stoppa, M., & Chiolerio, A. (2014). Wearable Electronics and smart textiles: A critical review. *Sensors*, 14(7), 11957–11992. <https://doi.org/10.3390/s140711957>
2. Kim, Y., Kim, J., Chicas, R., Xiuhtecutli, N., Matthews, J., Zavanelli, N., Kwon, S., Lee, S. H., Hertzberg, V. S., & Yeo, W. (2022). Soft wireless bioelectronics designed for real-time, Continuous Health Monitoring of farmworkers. *Advanced Healthcare Materials*, 11(13). <https://doi.org/10.1002/adhm.202200170>
3. Ban, S., Lee, Y. J., Kwon, S., Kim, Y.-S., Chang, J. W., Kim, J.-H., & Yeo, W.-H. (2023). Soft wireless headband bioelectronics and electrooculography for persistent human–machine interfaces. *ACS Applied Electronic Materials*, 5(2), 877–886. <https://doi.org/10.1021/acsaelm.2c01436>
4. Kang, T. W., Lee, J., Kwon, Y., Lee, Y. J., & Yeo, W. (2024). Recent progress in the development of flexible wearable electrodes for electrocardiogram monitoring during exercise. *Advanced NanoBiomed Research*, 4(8). <https://doi.org/10.1002/anbr.202300169>

5. Xu, S., Zhang, Y., Jia, L., Mathewson, K. E., Jang, K.-I., Kim, J., Fu, H., Huang, X., Chava, P., Wang, R., Bhole, S., Wang, L., Na, Y. J., Guan, Y., Flavin, M., Han, Z., Huang, Y., & Rogers, J. A. (2014). Soft microfluidic assemblies of sensors, circuits, and radios for the skin. *Science*, 344(6179), 70–74. <https://doi.org/10.1126/science.1250169>
6. Pan, J., & Tompkins, W. J. (1985). A real-time QRS detection algorithm. *IEEE Transactions on Biomedical Engineering*, 32(3), 230–236.
7. Clifford, G. D., Azuaje, F., & McSharry, P. (2006). Advanced Methods and Tools for ECG Data Analysis. Artech House.
8. Moody, G. B., & Mark, R. G. (2001). The impact of data preprocessing in the development of clinical ECG analysis algorithms. *IEEE Transactions on Biomedical Engineering*, 48(5), 499–506. <https://doi.org/10.1109/10.915647>
9. Inan, O. T., Migeotte, P. F., Park, K. S., Etemadi, M., Tavakolian, K., Casanella, R., & Di Rienzo, M. (2015). Wearable Ballistocardiography and Seismocardiography: A Review. *IEEE Journal of Biomedical and Health Informatics*, 19(4), 1414–1427. <https://doi.org/10.1109/JBHI.2014.2361732>
10. Aziz, S., Ahmed, S., & Alouini, M.-S. (2021). ECG-based machine-learning algorithms for Heartbeat classification. *Scientific Reports*, 11(1). <https://doi.org/10.1038/s41598-021-97118-5>
11. Acharya, U. R., Fujita, H., Lih, O. S., Adam, M., Tan, J. H., & Chua, C. K. (2017). Automated detection of arrhythmias using different intervals of tachycardia ECG segments with convolutional neural networks. *Information Sciences*, 405, 81–90. <https://doi.org/10.1016/j.ins.2017.04.012>
12. Hannun, A. Y., Rajpurkar, P., Haghpanahi, M., Tison, G. H., Bourn, C., Turakhia, M. P., & Ng, A. Y. (2019). Cardiologist-level arrhythmia detection and classification in ambulatory electrocardiograms using a deep neural network. *Nature Medicine*, 25(1), 65–69. <https://doi.org/10.1038/s41591-018-0268-3>
13. Casa, D. J., Clarkson, P. M., & Roberts, W. O. (2005). Exercise-Induced Heat Stress and Cardiovascular Strain: Importance of Hydration. *American Journal of Sports Medicine*, 33(5), 1123–1130. <https://doi.org/10.1177/0363546504274125>
14. Montain, S. J., & Coyle, E. F. (1992). Influence of graded dehydration on hyperthermia and cardiovascular drift during exercise. *Journal of Applied Physiology*, 73(4), 1340–1350. <https://doi.org/10.1152/jappl.1992.73.4.1340>
15. Casa, D. J., Armstrong, L. E., Hillman, S. K., Montain, S. J., Reiff, R. V., Rich, B. S., & Stone, J. A. (2000). National Athletic Trainers' Association Position Statement: Fluid replacement for athletes. *Journal of Athletic Training*, 35(2), 212–224. <https://www.ncbi.nlm.nih.gov/pmc/articles/PMC1323420/>
16. Vargas, N. T., & Marino, F. E. (2016). Superior heart rate variability and lower ventilatory response to exercise in athletes: Associations with hydration status and temperature regulation. *Physiology & Behavior*, 165, 276–283. <https://doi.org/10.1016/j.physbeh.2016.08.008>
17. Noakes, T. D. (2003). Fluid replacement during exercise. *Exercise and Sport Sciences Reviews*, 31(2), 130–135. <https://doi.org/10.1097/00003677-200304000-00010>

18. Armstrong, L. E. (2007). Assessing hydration status: The elusive gold standard. *Journal of the American College of Nutrition*, 26(Suppl 5), 575S-584S. <https://doi.org/10.1080/07315724.2007.10719661>
19. Almeida, M., Bottino, A., Ramos, P., & Araujo, C. G. (2019). Measuring heart rate during exercise: From artery palpation to monitors and apps. *International Journal of Cardiovascular Sciences*, 32(4), 396–407. <https://doi.org/10.5935/2359-4802.20190061>
20. Savvides, A., Giannaki, C. D., Vlahoyiannis, A., Stavrinou, P. S., & Aphamis, G. (2020). Effects of Dehydration on Archery Performance, Subjective Feelings and Heart Rate during a Competition Simulation. *Journal of Functional Morphology and Kinesiology*, 5(3), 67. <https://doi.org/10.3390/jfmk5030067>
21. Shephard, R. J. (2007). American College of Sports Medicine Position Stand: Exercise and Fluid Replacement. *Yearbook of Sports Medicine*, 2007, 254–255. [https://doi.org/10.1016/s0162-0908\(08\)70206-x](https://doi.org/10.1016/s0162-0908(08)70206-x)
22. Weiner, I. D., & Wingo, C. S. (1998). Hyperkalemia. *Journal of the American Society of Nephrology*, 9(8), 1535–1543. <https://doi.org/10.1681/asn.v981535>